Acta Cryst. (1998). D**54**, 306–312

1.2 Å Refinement of the Kunitz-Type Domain from the α3 Chain of Human Type VI Collagen

KARINE MERIGEAU,[a] BERNADETTE ARNOUX,[a] DAVID PERAHIA,[b] KJELD NORRIS,[c] FANNY NORRIS[c] AND ARNAUD DUCRUIX[a]*

[a]*Laboratoire d'Enzymologie et Biochimie Structurales, CNRS, 91198 Gif sur Yvette CEDEX, France,* [b]*Laboratoire de Modélisation et d'Ingenierie des Protéines, Université Paris-Sud, Bâtiment 430, 91405 Orsay CEDEX, France, and* [c]*Health Care Discovery, Novo Nordisk A/S, DK-2820 Gentofte, Denmark. E-mail: ducruix@lebs.cnrs-gif.fr*

(Received 13 December 1996; accepted 4 August 1997)

Abstract

The recombinant Kunitz-type domain (C5) of human collagen α3(VI) chain was previously described at 1.6 Å resolution at room temperature. By changing the crystallization conditions and using synchrotron radiation, we are able to record diffraction data to 1.2 Å resolution for crystals of the same space group at 291 K. The protein–water–ion model has been refined anisotropically against these new data using the program *SHELXL*93; the results converged to an *R* factor of 15.0%, with all data between 7 and 1.2 Å. The final electron-density map reveals a clear chain tracing with a few disordered residues and five residues out of 58 that present alternate conformations. The Cys14–Cys38 bond presents the less frequently observed left-hand conformation ($\chi_1 = -60°$). The solvent molecules and a phosphate ion are well ordered with an average *B* of 38 Å^2. The high-resolution structure reveals the N and C termini which were missing from the 1.6 Å structure.

1. Introduction

Kunitz-type modules are structural domains composed of a twisted antiparallel double-stranded β-structure bordered by two α-helices corresponding to the N and C termini. This structure is stabilized by 3 disulfide bridges, two of which are buried in the hydrophobic face of the molecule. First identified in protease inhibitors such as bovine pancreatic trypsin inhibitor (BPTI), the fold was also observed in a neural amyloid precursor protein (APPI) (Kitaguchi *et al.*, 1988; Ponte *et al.*, 1988; Tanzi *et al.*, 1988). Both BPTI and APPI share a common *P*1 site and a glycine in position 36, features characteristic of antiproteases.

Recently it has been shown (Chu *et al.*, 1990) that the C-terminus domain (C5) of the collagen α3(VI) chain exhibits a homologous sequence to Kunitz-type domain. The first 58 residues of the C-terminus domain of C5 were cloned and expressed in *Saccharomyces cerevisae* (Arnoux *et al.*, 1995) following conditions described for APPI (Petersen *et al.*, 1994). In terms of sequence (Fig. 1), the arginine residue in position *P*1 in C5 and APPI could potentially give them an antiprotease activity. This prediction was confirmed for APPI (Van Nostrand *et al.*, 1995) but not for C5. C5 has no inhibitory activity against trypsin, chymotrypsin, thrombin, kallikrein, neutrophile elastase, cathepsin G, factor VIIa or Xa (Petersen, unpublished results) or against mast cell chymase (Mayer *et al.*, 1994). This is not a result of proteolysis because C5 is not cleaved by trypsin even at high concentrations of enzyme (Bjorn, unpublished results).

1.1. *Comparison with other Kunitz fragments*

The structure of the C5 fragment was solved at 1.6 Å resolution by X-ray crystallography (Arnoux *et al.*, 1995) and more recently its solution structure has been analyzed by NMR (Zweckstetter *et al.*, 1996). From the *P′* cleavage side (residues 16–18), the aromatic Phe17 group, which is not conserved in BPTI and APPI, is buried in an hydrophobic pocket composed of Trp34, Tyr35 and Gly36. This unusual position of Phe17 forces the carbonyl group of residue 16 and the backbone N atom of residue 17 to rotate by more than 90°. This is not enough to prevent the inhibitory activity because the second domain of TFPI, the structure of which (Birktoft *et al.*, 1993) shows the same conformation as C5 for residues 16 and 17 (Petersen *et al.*, 1996), inhibits trypsin.

From the *P* side of this 'active loop' (12–14) two main differences should be noticed. Concerning the disulfide bridge (Cys14–Cys18): in the C5 structure, this bond shows a less frequently observed left-hand conformation ($\chi_1 = -60°$) in contrast with the major right one ($\chi_1 = +60°$) in BPTI (Srinivasan *et al.*, 1990). Because of this minor left position the constraint between Sγ Cys38 and the main chain is decreased and the N atom of Cys38 can form a hydrogen bond to the carbonyl O atom of Thr13 which adopts a position opposite of that observed in the APPI and BPTI structures. In BPTI, the mutation G36S (Otting *et al.*, 1993) induces a shift from the major right conformation to the minor left one for the disulfide bond 14–38. However, the G36S BPTI mutant maintains its inhibiting capability toward the serine proteinases, and in the G36S mutant the hydroxyl group replaces one of the four internal water molecules and stabilizes the minor left conformation.

ISSN 0907-4449

Table 1. *Crystallization conditions and data collection parameters of the two crystals of C5*

	Crystal 1	Crystal 2
Buffer of crystallization	0.2 *M* lithium sulfate 0.1 *M* citric acid 0.074 *M* disodium hydrogen phosphate pH 3.3	
Precipitating agent	1.6 *M* ammonium sulfate	
Concentration of protein (mg ml^{-1})	10	9
Space group	$P2_1$	
Lattice constants (Å, °)		
a	25.69	25.87
b	38.04	38.28
c	28.64	28.84
β	109.20	109.04
% Solvent	39	
Crystal size (mm)	2 × 0.4 × 0.4	1 × 0.2 × 0.2
Resolution (Å)	6.9–1.18	20.6–1.50
Total No. of reflections	53121	34459
Wavelength (Å)	0.901	0.9375
Crystal–detector (mm)	150	120
Scan rate (° min^{-1})	0.25	
θ range (°)	0–180	

1.2. *How can antiprotease activity be recovered?*

A tentative modelling of the complex between C5 and trypsin (Arnoux *et al.*, 1995) led to the conclusion that the residues located in *P*3, *P*1′ and *P*2′ (13, 16 and 17) appear to be responsible for this non-antiprotease activity. The carbonyl O atom of Thr13 in C5, which has a different conformation from that of Pro13 in BPTI prevents the formation of a crucial hydrogen bond between O Thr13 and N Gly216 of trypsin which occurs in BPTI/trypsin complex. However the single mutation T13P does not transform C5 to a proteinase inhibitor (no detectable inhibition activity toward trypsin), in contrast to the results with D16A (K_d = 250 n*M*) (Kohfeldt *et al.*, 1996). Each of the other single mutations requires the presence of an alanine residue in position 16 to inhibit the enzyme. This highlights the importance of the presence of an alanine in *P*1′. The negative charge carried by the carboxylate group of Asp16 on the surface of C5 is not present in BPTI; in this protein the residue is alanine. The negative charge of Asp16 is not compatible with the presence of Asp189 from the catalytic pocket of trypsin.

The rotation of the carbonyl residue of Asp16 is induced by Phe17 which prevents hydrogen bonding between the main-chain N atom of Phe17 and the carbonyl O atom of Phe41 of trypsin. The orientation of the phenyl ring of Phe17 in C5 structure would cause a van der Waals contact violation with main-chain atoms of Gln192 and Gly193 of trypsin (Fig. 2). It would also cause a short contact distance between the carbonyl group of Asp16 (C5) and histidine 57 of the catalytic triad of trypsin. Because Phe17 of C5 is buried in a hydrophobic pocket, the single mutation F17R would not be sufficient to restore the inhibitory activity because it does not allow the formation of a hydrogen bond between the guanidinium group of Arg17 (C5) and the active site of trypsin. However, the W34V mutation, would allows for the χ_1 rotation of Phe17 and the release of van der Waals contact constraint. This explains why a double mutation is essential for the restoration of activity. Based on the crystallographic and NMR studies, various mutations were studied by two groups. The double mutants D16A-F17R and D16A-T13P (Kohfeldt *et al.*, 1996), D16A-R15K (Norris, unpublished data) present a K_D of 2.8, 11.45 n*M*, respectively. Finally triple mutations (Kohfeldt *et al.*, 1996) D16A-T13P-F17R (K_D = 0.023 n*M*) and D16A-T13P-W34V (K_D = 0.046 n*M*) fully restore trypsin inhibition with the same activity as BPTI (K_D = 0.031 n*M*).

Because the NMR study demonstrated that C5 is a highly dynamic molecule at room temperature, with multiple conformers which could not be properly located in the 1.6 Å resolution X-ray structure (Arnoux *et al.*, 1995), we have measured a new X-ray diffraction data set at room temperature using wiggler beam synchrotron radiation. We refined the structure using *SHELXL*93 program (Sheldrick, 1993) at 1.2 Å resolution, which allowed for anisotropic refinement.

2. Experimental

2.1. *Crystal and crystallographic data collection*

The protocol initially devised by F. Norris (Arnoux *et al.*, 1995), was modified in the following way: the pH was changed to 3.3, the temperature was 291 K and the protein concentration was higher (Table 1). Two crystals were used to record data at 291 K using station DW32 (Fourme *et al.*, 1992) at LURE with an incident wavelength close to 0.9 Å. Data up to 1.18 Å were recorded using two crystals of C5 fragment, and were processed using the *MOSFLM* program (Leslie, 1987), and merged (Table 2) using the *ROTAVATA/AGROVATA*

```
          5    10    15    20    25    30    35    40    45    50    55
C5:   ETDICKLPKDEGTCRDFILKWYYDPNTKSCARFWYGGCGGNENKFGSQKECEKVCAPV

APPI:VREVCSEQAETGPCRAMISRWYFDVTEGKCAPFFYGGCGGNRNNFDTEEYCMAVCGSA

BPTI:RPDFCLEPPYTGPCKARIIRYFYNAKAGLCQTFVYGGCRAKRNNFKSAEDCMRTCGGA

DEND:RRKLCILHRNPGRCYDKIPAFYYNQKKKQCEHFDWSGCGGNSNRFKTIEECRRTCIG
```

Fig. 1. Alignment of the amino-acid sequences of C5, APPI, BPTI and dendrotoxin. Cysteine residues involved in disulfide bridges are printed in bold.

Table 2. *Statistical parameters of the two C5 data sets*

Data set	Resolution range (Å)	No. of unique reflections	Multiplicity	$\langle I\rangle/\langle\sigma\rangle$	Completeness (%)	No. of overlapping reflections	R_{sym}
1	6.9–1.18	16216	3.2	4.4	94.1		0.075
2	20.6–1.50	8300	3.7	5.3	96.2		0.034
Merged 1 + 2	20.45–1.18	16657	4.9	3.6	97.1	6486	R_{merge} 0.055

programs as implemented in the *CCP*4 suite of programs (Collaborative Computational Project, Number 4, 1994). A total of 84 000 reflections were processed to yield 16 657 unique reflections with an overall R_{merge} of 5.5%. At the limit of resolution, data were 96% complete at 1.2 Å and 61% of the outer shell reflections have $I > 2\sigma(I)$. The overall *B* factor deduced from the Wilson plot slope is 21.7 Å^2 between 22 and 1.2 Å.

2.2. *Refinement*

2.2.1. *X-PLOR 3.1.* Refinement was started from the isotropically refined coordinates (PDB entry 1KNT) containing 440 non-H atoms, 43 water molecules and a sulfate ion. At this stage, the N-terminal Glu1 residue and the C-terminal Pro57 and Val58 residues were not available because no electron density was visible in the 1.6 Å map. The 1.2 Å data set contained 16 657 reflections of which 1631 were isolated to calculate the R_{free} factor as defined by Brünger (Brünger, 1992). The protein–water–ion model was first refined using *X-PLOR* 3.1 (Kuriyan *et al.*, 1991). Because a new data set was used, a few cycles of rigid-body refinement were carried out at 1.6 Å resolution followed by 200 cycles of Powell minimization using individual *B* factors. At this stage, the *R* factor was 22.8% and the R_{free} was 30.6%. Then the resolution was increased step by step from 1.6 to 1.4 Å and finally to 1.2 Å including each time 200 cycles of conjugated gradient minimization which brought the *R* factor down to 22.4% and the R_{free} to 26.7%. It is interesting to note that a parallel refinement using the *RESTRAIN* program (Driessen *et al.*, 1989) led to similar results.

2.2.2. *SHELXL93.* The *X-PLOR* coordinate file was converted to the *SHELXL*93 format using the *PDBINS* program, whereas the reflection file was converted using the *F2MTZ* program. 10% of the data were set aside to calculate an R_{free}. The procedure for selecting these 10% of reflections is different from that in *X-PLOR*; instead of a random extraction of 10%, every tenth reflection was selected by the *SHELXL*93 program. A first run of conjugated-gradient least-squares refinement using isotropic *B* factors led, respectively, to an *R* factor of 20.7% and R_{free} of 24.7% with data from 7 to 1.2 Å resolution. Then all non-H atoms were given an anisotropic *B* factor and refinement was resumed. After ten cycles, R_{free} and the *R* factor were lowered to 22.2 and 16.2%, respectively, for 10 762 reflections greater than 4σ. Analysis of the electron-density map revealed alternate conformers for residues (Thr2, Asp3, Thr13, Asp16, Ile18). Two of them (Thr13, Ile18) were already observed at 1.6 Å resolution, but were not stable enough to be refined. Moreover, clear electron-density peaks appeared at the locations of the missing residues 1, 57 and 58. New conformers and residues were introduced in the refinement, first with isotropic *B* factors.

In the 1.6 Å refinement a sulfate ion was included in the model. Phosphate or sulfate ions present the same geometry with respect to their angles even if P—O bonds (1.56 Å) are longer than S—O bonds (1.42 Å). Because of higher resolution data, we tried to discri-

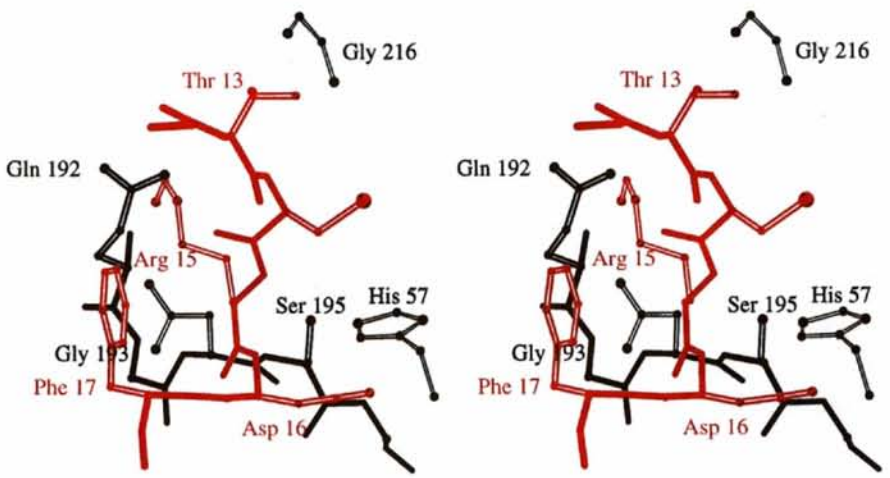

Fig. 2. Modeling of Phe17 environment of C5 (red) superimposed with the BPTI molecule of the trypsin (black)/BPTI (blue) complex (2PTC) showing prohibited van der Waals contacts.

minate between P and S atoms, although they differ by only one electron. Both independent refinement cycles, with unrestrained constants for the anion atoms, led to an average bond length $X-O$ of 1.55 Å, which is in favor of a phosphate ion included in the coordinate file.

The last refinement cycle led to an R factor of 13.6% for 10 762 reflections greater than 4σ (7–1.2 Å) and an R_{free} of 20.5%. Including all reflections (16 307), the value of the R factor is 15.0% between 7 and 1.2 Å. The average calculated B factor for the protein is 21 Å^2. It is to be noted that there is a shift (8 Å^2) from the 1.6 Å refinement using *X-PLOR*3.1, which is probably due to the change of program used in the refinement.

2.3. *The normal mode calculation*

The crystal structure was progressively minimized with 100 steps of conjugate gradient followed by 7000 cycles with the *ABNR* algorithm (Brooks *et al.*, 1983). The minimization protocol was chosen so that the structure can relax without allowing it to deviate too much from the initial structure. All the calculations were performed with the *CHARMM* molecular modeling program (Brooks *et al.*, 1983) using all-hydrogen parameter set 22. Electrostatic interactions were calculated up to an interatomic distance of 11 Å using a shift function.

3. Results and discussion

3.1. *Final model*

Anisotropic refinement led to the final model which has a good geometry. The estimate average errors on the coordinates is 0.1 Å, a value obtained either by the Luzzati plot or the *SIGMAA* program. The final model is composed of 532 non-H atoms, 51 water molecules and one phosphate ion. The electron density is very well defined for all the atoms of the main chain. All the

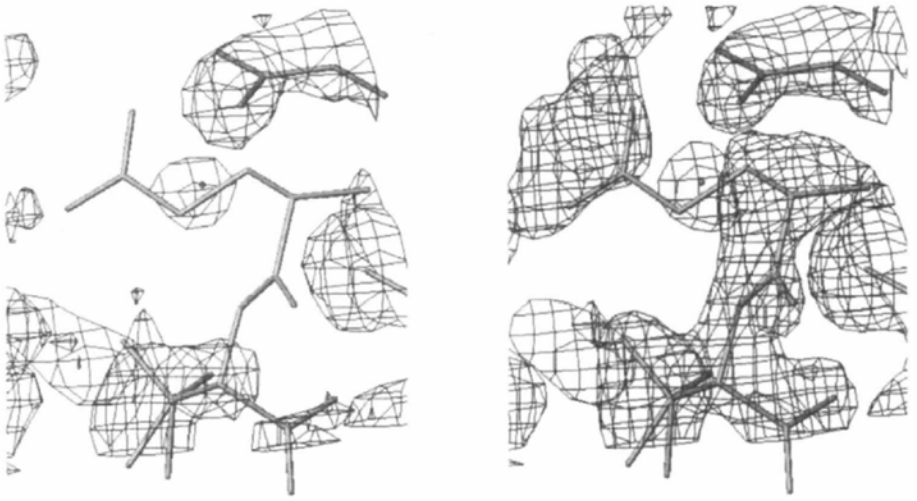

(*a*)

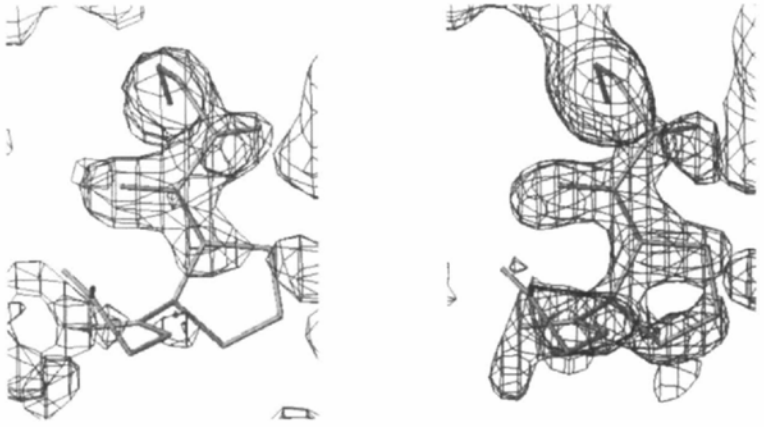

(*b*)

Fig. 3. (*a*) N-terminal Glu1 residue and (*b*) C terminal (Pro57, Ala58) residues in the $2F_o - F_c$ electron-density map (1σ), before (left) and after (right) refinement at 1.2 Å resolution. Drawings were produced using the *O* program (Jones, 1978).

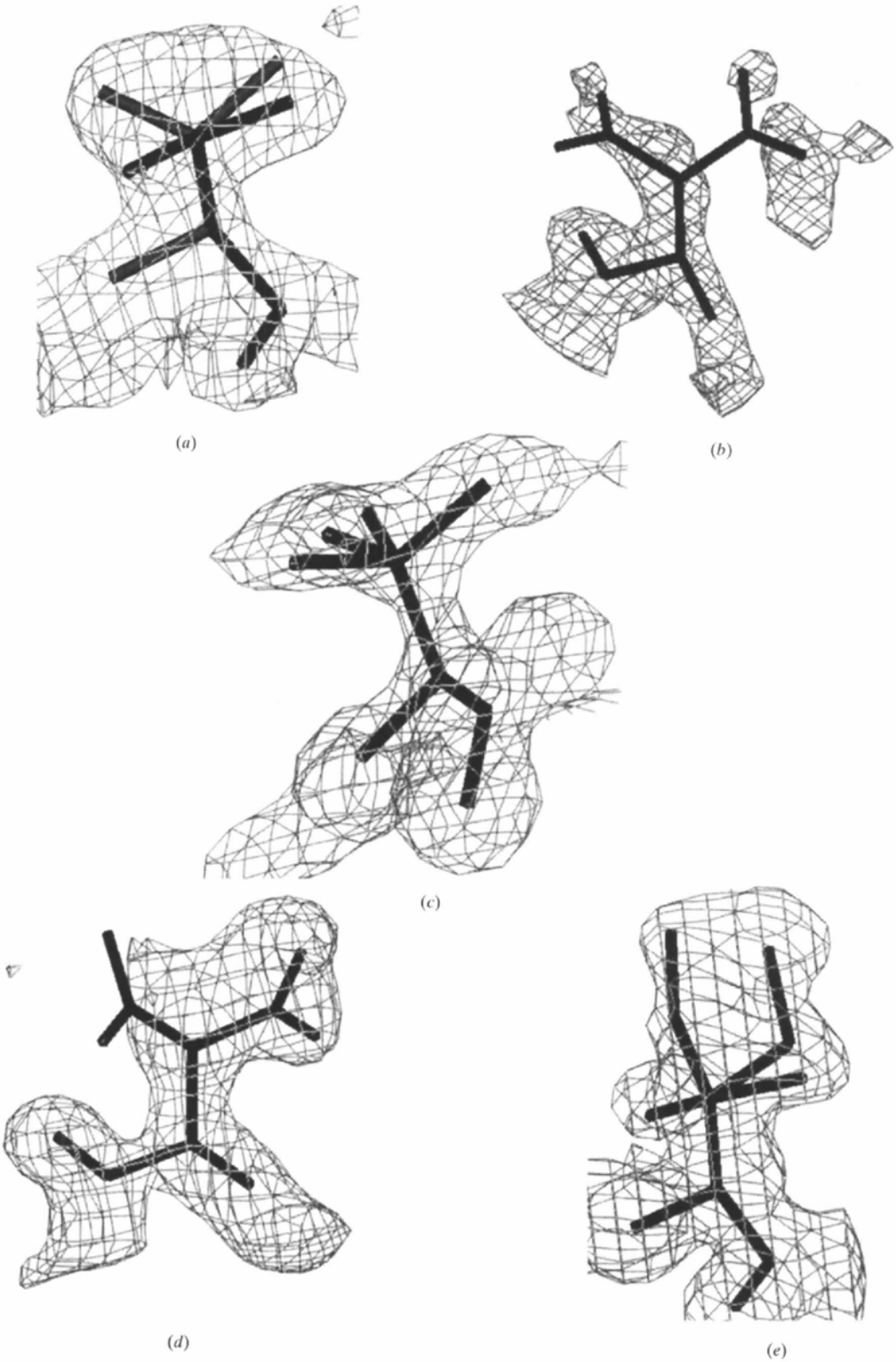

Fig. 4. Alternate conformations of (*a*) Thr2, (*b*) Asp3, (*c*) Thr13, (*d*) Asp16 and (*e*) Ile18 deduced from the $2F_o - F_c$ electron-density map (1σ).

residues are found in the favorable regions of the Ramachandran plot except for Cys14, the conformation of which will be discussed below. It is clear, however, that the refinement is at the frontier between isotropic and anisotropic refinement. Data obtained at cryogenic temperature may lead to a better resolution.

3.2. *Comparison with the 1.6 Å structure*

The protein scaffold has not changed during this refinement at higher resolution, the r.m.s. is 0.1 Å for all Cα atoms between the two models. However, residues Pro57 and Glu1, which were not previously observed in the electron-density map at 1.6 Å resolution, have been traced without ambiguity, although the electron density fades past Cγ of Glu1 (Fig. 3). The main-chain electron density of Val58 is weak, and its side chain was not located.

Alternate conformers have been introduced for side chains of Thr2, Asp3, Thr13, Asp16 and Ile18 (Fig. 4). The last three residues belong to the binding loop corresponding to the P' side of BPTI. It has been postulated (Arnoux *et al.*, 1995) that the absence of antiprotease activity of C5 can be due to a 180° rotation of the carbonyl group of Asp16 and the backbone N atom of Phe17. Phe17 probably does not have alternate conformations because it is buried in a hydrophobic pocket consisting of Trp34, Tyr35, Gly36 and a few backbone C atoms. These conformations have also been observed in the second Kunitz domain of the tissue factor pathway inhibitor (TFPI) (Petersen *et al.*, 1996). Side chains of Lys28, Lys49 and Glu42 have very large thermal motion, but they were not consistent with alternate stable conformers. The percentage of residues presenting alternate conformations is in total agreement with that observed in other structures refined at atomic resolution (Dauter *et al.*, 1995).

3.3. *Solvent*

During the 1.2 Å resolution refinement it was possible to include 10% more water molecules than in the 1.6 Å model. Because of the noncryogenic temperature used during data measurement, this percentage is obviously less than for a structure refined at 150 K or lower temperatures. Nevertheless a network of water molecules could be observed surrounding the protein; some of them belong to the second hydration shell. The average number of hydrogen bonds to a water molecule is two. Two water molecules are buried and present no contact with the bulk solvent. These two water molecules lie in a pocket between residues 8–10 and residues 40–44. These internal water molecules are tetrahedrally bonded and are found at the same location as two out of four found in the different structures of BPTI determined either by X-ray crystallography (Deisenhofer & Steigemann, 1975; Wlodawer, 1987) or NMR (Berndt *et al.*, 1992; Otting *et al.*, 1993).

3.4. *Phosphate or sulfate ion*

Phosphate ions location in X-ray structures have been reviewed (Chakrabarti, 1993) and recently implicated in a facilitation of crystal packing (Takahashi *et al.*, 1993). It is also reported that they can alter the relative stability of the protein, as shown by molecular dynamic simulations, mutational studies and the conservation of residues around the ion. These suggest a possible role for phosphate ions in stabilizing particular intermediates in the folding/unfolding process (Schiffer & van Gunsteren, 1996).

The location of the phosphate ion in the C5 structure, hereafter called site 1, is quite far from the one (site 2) presents in all crystal forms of BPTI. The BPTI ion phosphate is in the divalent form (HPO_4^{2-}) at neutral pH whereas, because of the pH 3.3 used during the crystallization process, the C5 phosphate ion is in the monovalent form ($H_2PO_4^-$). The latter settles in site 1 near Trp21. Any location of a phosphate ion in the same region of BPTI would correspond to a negatively charged region, but this would be incompatible with the negative charge of the phosphate ion. This may be linked to the overall negative charge ($-3\,e^-$) of APPI compared with the positive values for BPTI ($+6\,e^-$) at pH 7.0 and C5 ($+9\,e^-$) at pH 3.3. The absence of a phosphate ion at site 2 in the C5 structure is not due to a change of environment from that in BPTI, as it corresponds to a region which is as positive as the one occupied by the current C5 phosphate ion. Indeed, the requirement of Tyr35 for binding the phosphate ion is necessary as shown by the mutant Y35G (8PTI) which does not contain a phosphate ion.

3.5. *Analysis of normal mode calculations*

The energy minimization using the *CHARMM* program for the C5 structure was performed up to an energy gradient of 8×10^{-5} kcal mol^{-1} Å^{-1} (33.4×10^{-5} kJ mol^{-1} Å^{-1}). The r.m.s. coordinate deviation

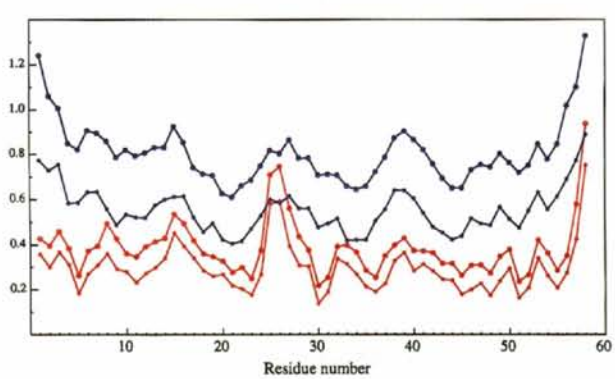

Fig. 5. Fluctuations (in Å) of Cα atoms obtained by the normal mode analysis (red) and by the anisotropic temperature factors (blue) analysis. Large dots indicate the total fluctuations and small ones to the largest component of the principal axes of fluctuations.

between the crystal structure and the minimized structure is 1.1 Å for the main-chain atoms and 1.39 Å for all atoms. This relatively large difference in three-dimensional structures is due to the fact that for the minimization, an isolated single molecule was considered without any consideration of crystal packing contacts. The fluctuation matrix of a given atom obtained by normal mode analysis was diagonalized to obtain the principal axes of fluctuations. The largest value and the total fluctuation obtained for each Cα atom were plotted (Fig. 5) as a function of residue number in order to get the extent of anisotropy in the fluctuations. The same kind of values obtained from the crystal anisotropic temperature factors were also presented for comparison. The normal mode results indicate fluctuations with a large anisotropy since the total fluctuations are close to the largest component of the principal axes of fluctuations. The anisotropy in the crystal fluctuations are less marked. However, a good correlation between the theoretical fluctuations and the X-ray profiles are observed. The largest fluctuations are obtained for the 7–10, 14–18, 24–28, 31–35 and 54–58 regions in both analyses, but the normal mode fluctuations obtained for the 24–28 region is more pronounced than in the crystal case. This could be explained by the analysis of crystal packing. The 24–28 region of the minimized structure can be easily superimposed on the refined 1.2 Å structure of C5 by a single rigid-block rotation of this loop. Its position is shifted toward the center of the molecule due to the presence of the Thr2 residue belonging to the N-terminus domain of a symmetry-related molecule in the crystal structure.

A more detailed analysis of the normal modes showed that the large fluctuations observed for the 15–18 and 24–29 regions are mainly contributed to by the first two lowest frequency normal modes (5.4 and 6.2 cm^{-1}). The fluctuation of the region 9–12 is mainly contributed to by the third lowest frequency modes (7.1 cm^{-1}). These regions display a large motion along preferred directions as given by these lowest frequency modes.

We are grateful to R. Fourme and J. P. Benoit for the development of the W32 station at LURE. We acknowledge the financial support from the Centre National de la Recherche Scientifique.

References

Arnoux, B., Mérigeau, K., Saludjian, P., Norris, F., Norris, K., Bjorn, S., Olsen, O., Petersen, L. & Ducruix, A. (1995). *J. Mol. Biol.*, **246**, 609–617.

Berndt, K. D., Güntert, P., Orbons, L. P. M. & Wüthrich, K. (1992). *J. Mol. Biol.* **277**, 757–775.

Birktoft, J., Norris, F., Kelly, C. A. & Norris, K. (1993). *Thromb. Haemostasis*, **69**, 679.

Bode, W., Turk, D. & Karshikov, A. (1992). *Protein Sci.* **1**, 426–471.

Brooks, B. R., Bruccoleri, R. E., Olafson, B. D., States, D. J., Swaminathan, S. & Karplus, M. (1983). *J. Comput. Chem.* **4**, 187–217.

Brünger, A. T. (1992). *Nature (London)*, **355**, 472–475.

Collaborative Computational Project, Number 4 (1994). *Acta Cryst.* D**50**, 760–763.

Chakrabarti, P. (1993). *J. Mol. Biol.* **234**, 463–482.

Chu, M.-L., Zhang, R.-Z., Pan, T.-C., Stokes, D., Conway, D., Kuo, H.-J., Glanville, R., Mayer, U., Mann, K., Deutzmann, R. & Timpl, R. (1990). *EMBO J.* **9**, 385–393.

Dauter, Z., Lamzin, V. S. & Wilson, K. S. (1995). *Curr. Opin. Struct. Biol.* **5**, 784–790.

Deisenhofer, J. & Steigemann, W. (1975). *Acta Cryst.* B**31**, 238–250.

Driessen, H. P. C., Haneef, I., Harris, G. W., Howlin, B., Khan, G. & Moss, D. S. (1989). *J. Appl. Cryst.* **22**, 510–516.

Fourme, R., Dhez, P., Benoit, J.-P., Kahn, R., Dubuisson, J.-M., Besson, P. & Frouin, J. (1992). *Rev. Sci. Instrum.* **63**, 982–987.

Jones, T. A. (1978). *J. Appl. Cryst.* **11**, 268–272.

Kitaguchi, N., Takahashi, Y., Tokushima, Y., Shiojiris, S. & Ito, H. (1988). *Nature (London)*, **331**, 530–532.

Kohfeldt, E., Göhring, W., Mayer, U., Zweckstetter, M., Holak, T. A., Chu, M.-L. & Timpl, R. (1996). *Eur. J. Biochem.* **238**, 333–340.

Kuriyan, J., Osapay, K., Burley, S. T., Brünger, A. T., Hendrickson, W. A. & Karplus, M. (1991). *Proteins Struct. Funct. Genet.* **10**, 340–358.

Leslie, A. G. W. (1987). *Proceedings of the CCP4 study weekend.* Warrington: Daresbury Laboratory.

Mayer, U., Pöschl, E., Nischt, R., Pan, T.-C., Chu, M.-L. & Timpl, R. (1994). *Eur. J. Biochem.* **225**, 573–580.

Otting, G., Liepinsh, E. & Wüthrich, K. (1993). *Biochemistry*, **32**, 3571–3582.

Petersen, L. C., Bjorn, S. E., Norris, K., Norris, F., Sprecher, C. & Foster, D. C. (1994). *FEBS Lett.* **338**, 53–57.

Petersen, L. C., Bjorn, S. E., Olsen, O. H., Nordfang, O., Norris, F. & Norris, K. (1996). *Eur. J. Biochem.* **235**, 310–316.

Ponte, P., Gonzales-DeWhitt, P., Schilling, J., Miller, J., Hsu, D., Greenberg, B., Davis, K., Wallace, W., Lieberburg, I., Fuller, F. & Cordell, B. (1988). *Nature (London)*, **331**, 525–527.

Schiffer, C. A. & van Gunsteren, W. F. (1996). *Proteins Struct. Funct. Genet.* **26**, 66–71.

Sheldrick, G. M. (1993). *SHELXL93: a program for the refinement of crystal structures.* University of Göttingen, Germany.

Srinivasan, N., Sowdhamini, C. & Balaram, P. (1990). *Int. J. Pept. Protein Res.* 147–155.

Tanzi, R. E., McClatchey, A. I., Lamperti, E. D. & Villaa-Komaroff, L. (1988). *Nature (London)*, **331**, 528–530.

Takahashi, T., Endo, S. & Nagayama, K. (1993). *J. Mol. Biol.* **234**, 421–432.

Van Nostrand, W. E., Schmaier, A. H., Siegel, R. S., Wagner, S. L. & Raschke, W. C. (1995). *J. Biol. Chem.* **270**, 22827–22830.

Wlodawer, A. (1987). *J. Mol. Biol.* **193**, 145–156.

Zweckstetter, M., Czisch, M., Mayer, U., Chu, M.-L., Zinth, W., Timpl, R. & Holak, T. A. (1996). *Structure*, **4**, 195–209.